Hydrogen Spillover on Carbon-Supported Metal Catalysts Studied by Inelastic Neutron Scattering. Surface Vibrational States and Hydrogen Riding Modes

Philip C. H. Mitchell,*,† Anibal J. Ramirez-Cuesta,†,‡ Stewart F. Parker,‡ John Tomkinson,‡ and David Thompsett§

Department of Chemistry, University of Reading, Reading RG6 6AD, U.K., ISIS Facility, Rutherford Appleton Laboratory, Chilton, Didcot OX11 0QX, U.K., Johnson Matthey Technology Centre, Sonning Common, Reading RG4 9NH, U.K.

Received: December 16, 2002; In Final Form: April 28, 2003

Hydrogen spillover on carbon-supported precious metal catalysts has been investigated with inelastic neutron scattering (INS) spectroscopy. The aim, which was fully realized, was to identify spillover hydrogen on the carbon support. The inelastic neutron scattering spectra of Pt/C, Ru/C, and PtRu/C fuel cell catalysts dosed with hydrogen were determined in two sets of experiments: with the catalyst in the neutron beam and, using an annular cell, with carbon in the beam and catalyst pellets at the edge of the cell excluded from the beam. The vibrational modes observed in the INS spectra were assigned with reference to the INS of a polycyclic aromatic hydrocarbon, coronene, taken as a molecular model of a graphite layer, and with the aid of computational modeling. Two forms of spillover hydrogen were identified: H at edge sites of a graphite layer (formed after ambient dissociative chemisorption of H_2), and a weakly bound layer of mobile H atoms (formed by surface diffusion of H atoms after dissociative chemisorption of H_2 at 500 K). The INS spectra exhibited characteristic riding modes of H on carbon and on Pt or Ru. In these riding modes H atoms move in phase with vibrations of the carbon and metal lattices. The lattice modes are amplified by neutron scattering from the H atoms attached to lattice atoms. Uptake of hydrogen, and spillover, was greater for the Ru containing catalysts than for the Pt/C catalyst. The INS experiments have thus directly demonstrated H spillover to the carbon support of these metal catalysts.

Introduction

We report a study of hydrogen spillover on carbon-supported metal catalysts using inelastic neutron scattering. Our aim has been to detect and quantify the spillover hydrogen.

Metal catalysts consist of metal particles supported on high surface oxide or carbon. Many catalytic reactions involve hydrogen,[1] and spillover of hydrogen is often implicated.[2] In spillover, hydrogen atoms, produced by dissociative chemisorption of dihydrogen on the metal part of a catalyst, diffuse from the metal to the catalyst support. On an oxide-supported metal catalyst, spillover hydrogen atoms react with the oxide forming OH species that can be identified by infrared spectroscopy.[3] On a carbon-supported catalyst, spillover hydrogen may bind, for example at unsaturated edge sites, or constitute a layer of weakly bound, mobile hydrogen atoms. Direct detection of spillover hydrogen on carbon is problematical.[4] We have adopted a fresh approach to the problem using inelastic neutron scattering (abbreviated INS) spectroscopy.

Neutrons are scattered by all atomic nuclei, but in incoherent inelastic scattering (which is the type of scattering here), the scattering is from single centers and so there can be no interference of scattered waves. Neutrons lose energy by exciting vibrational modes of the scatterer; the INS spectrum is an energy loss spectrum. The spectrum is a vibrational spectrum of a substance over the range 16−4000 cm^{-1} with a resolution of 1−1.5% of the energy transferred ($\Delta E/E$). All molecular vibrations are neutron-active because the nuclear interactions are not subject to dipole or polarizability selection rules and all vibrations are therefore, in principle, observable. The scattering intensity is proportional to the concentration of the scatterer and its cross section. Because the scattering cross section is much greater for hydrogen (80 barn) than for any other element (5 barn), displacements involving hydrogen dominate in neutron spectroscopy. The neutron is an ideal probe for the study of hydrogen in catalysts.[5]

From adsorption of hydrogen on a carbon-supported metal catalyst, we might expect any or all of these species, all of which are identifiable by INS: (1) adsorbed dihydrogen molecules, (2) H bound to the metal, (3) spillover H atoms strongly bound to previously unsaturated carbon atoms, probably at edge sites or basal plane defects, and (4) spillover H weakly bound to the carbon and mobile.

We have previously studied H_2 on Ru/C[6] and cobalt aluminum phosphate.[7] Here we shall see that adsorbed H_2 molecules are detected after hydrogen adsorption only at a low temperature, for example, 77 K.

The interaction of H with metal particles, free or supported, has been much studied. Platinum−hydrogen vibrational modes have been assigned in the INS spectrum of a hydrogen-dosed Pt/C catalyst similar to ours.[8]

The interaction of hydrogen with carbon and graphite has been studied experimentally and computationally.[9] The potential energy surface for a H atom approaching a carbonaceous surface has been calculated using the polycyclic aromatic hydrocarbon coronene (see later) as a model of graphite.[10] There were two

* Corresponding author. E-mail: p.c.h.mitchell@reading.ac.uk.
† University of Reading.
‡ Rutherford Appleton Laboratory.
§ Johnson Matthey Technology Centre.

10.1021/jp0277356 CCC: $25.00
Published on Web 06/20/2003

TABLE 1: Properties of the Catalysts

	Pt/C	Ru/C	PtRu/C-01
composition/[mol M (g cat)$^{-1}$]	0.002	0.002	0.001 + 0.001
M crystallite size (X-ray)/nm	4.0	3.4	1.9
M surface area (CO)/(m^2 g^{-1})	63	180	139

adsorption regions separated by a barrier: a physisorption region having mobile H atoms translating parallel to the surface, and a chemisorption region having H bound on top of a carbon atom. That work and later work[11] are pertinent to this study. We have, therefore, repeated and confirmed the results of these calculations and also calculated the interaction of H atoms with graphite. Further, we have measured and calculated the INS spectra of the polycyclic aromatic hydrocarbon coronene to validate the computational model.

INS is not, in itself, a surface technique. The mean free path of a thermal neutron in matter is ~1 cm; neutrons easily penetrate a substance, and so an INS spectrum is the sum of the spectra representing the scattering of neutrons deep in the bulk of a substance and at the surface.[12] We see surface scattering (1) when a substance has a large surface-to-volume ratio s/v (number of atoms, N, in a 20−30 nm particle ≤ 105, 20−30 nm average size, surface area ~ 20 m^{2}g^{-1}), (2) when the surface composition differs from the bulk composition, in particular when the surface is hydrogenated or protonated much more than the bulk, and (3) from adsorbed species, especially when they are hydrogenous. Once again, we exploit the high neutron scattering cross section of hydrogen.

Surface vibrational modes of the substrate (the catalyst and the support) may appear as so-called *riding modes*; through these we can observe surface vibrational states by INS.[13−15] The surface modes are amplified by neutron scattering from surface-bound H atoms and so distinguished from the bulk modes of the substrate. The H atoms, whether free or combined, move in phase with the vibrations of the surface atoms (as a rider moves with their horse). For example, in the INS spectra of hydrogen on Pt black and of water on nickel particles, riding modes are observed which correlate with the surface vibrational modes of platinum[13,16] and nickel.[12,13]

In this paper we report the direct observation of spillover hydrogen on Pt/C, Ru/C, and PtRu/C fuel cell catalysts. Dihydrogen molecules dissociate on the Pt or Ru component of the catalyst, and H atoms spillover onto the carbon support. In a previous paper[17] we reported the characterization, also using inelastic neutron scattering, of slowly diffusing spillover hydrogen on a Pt/C catalyst. The spillover hydrogen diffused over macroscopic distances on the carbon support during a period of days, forming a layer of weakly bound mobile hydrogen atoms. In the present paper we expand on the earlier work and, in addition, describe spillover hydrogen, which appears on a carbon support within minutes of dosing the catalysts with hydrogen.

Experimental Section

Model Compounds. Coronene, $C_{24}H_{12}$ (**1**), 99%, was bought from Aldrich.

Catalysts. The catalysts were commercial high loading (40% metal) carbon-supported Pt and Ru fuel cell catalysts. The carbon support was a carbon black XC72. Properties of the catalysts are summarized in Table 1.

Sample Cells. Two designs of cell were used. The first, which is the design generally used for our INS experiments, we call the *standard sample cell*. These sample cells, which were used for catalyst pretreatment and dosing and for the neutron scattering measurements, were constructed from two circular, 85 mm diameter, stainless steel conflat blanks. A hollowed out region of one plate, 60 mm diameter, 10 mm depth, accommodated the catalyst; a second plate, thickness 1 mm, was bolted to the first with a seal provided by a copper gasket. The cells are equipped with gas inlet and outlet tubes, which could be connected to high vacuum and gas dosing equipment, and a thermocouple. The cell was tested to maintain a vacuum of 10^{-7} mbar and a pressure of 5 bar.

The second design of cell, which we call the *annular cell*,[17] made possible scattering of neutrons from hydrogen on the carbon without scattering from the catalyst. Arranged in an outer ring within the can are pellets of catalyst, Pt/C; they sit outside the neutron beam and are in contact with the central mass of carbon support. Only the central section is illuminated with the neutron beam. We could thus observe any spillover hydrogen on the carbon support alone.

Pretreatment and Dosing of the Catalyst. The catalyst (~10 g), loaded into the cell to be used in the neutron scattering experiments, was pretreated by heating to constant mass in a flowing 10 vol % H_2/He mixture at 373 K to remove superficial oxide and water, and it was evacuated to a constant 10^{-7} mbar. Release of water was monitored by sampling the outlet gas to a mass spectrometer. Reduction and evacuation of the catalysts were continued until no more water was observed.

The reduced and evacuated catalysts were dosed with pure hydrogen (99.999%) from a 1.0 l bottle at 1 bar, and the hydrogen uptake was monitored by the pressure change of hydrogen in the dosing bottle. Two lots of dosed catalyst were prepared: *slow-H-dosed catalysts*, using the annular cell for which hydrogen dosing was continued at temperatures up to 500 K for days, and *fast-H-dosed catalysts*, using the standard cell for which hydrogen dosing at 293 K was completed after ~5−30 min. Some catalysts were also dosed with hydrogen at 77 K.

Inelastic Neutron Scattering Spectra. Inelastic neutron scattering spectra of the empty sample cell, the carbon support, and the dihydrogen-dosed catalysts were recorded on the TOSCA spectrometer at the ISIS pulsed neutron source at the Rutherford Appleton Laboratory, Chilton, U.K.[18] TOSCA is a high resolution, broad range, inverse geometry spectrometer well suited to the spectroscopy of hydrogenous materials. The energy transfer range is from 16 to 8000 cm^{-1}. The resolution is $\Delta E/E$ ~ 1.5%. Spectra were recorded at ~20 K to freeze the chemistry and to reduce thermal effects that degrade the spectra. The spectra are presented as the scattering law $S(\boldsymbol{Q},\omega)$ (or function) (S, intensity; $\boldsymbol{Q}$, momentum transfer; ω, energy transfer) plotted versus energy transfer and were analyzed using the Origin data analysis package.[19] The INS spectra of the cell and of the catalyst before hydrogen dosing were first recorded: the *background spectrum*. Hydrogen was then admitted to the cell. When the hydrogen dosing had been completed, the temperature of the cell plus catalyst was lowered to ~20 K and the INS spectrum was then recorded: the *loaded spectrum*. To obtain the INS spectrum of just hydrogen on the catalyst, the *background spectrum* is subtracted from the *loaded spectrum*.

This procedure was tested to ensure that it introduced no artifacts. Samples of the catalyst were treated in the same cans with the same temperature program, but argon was used in place of hydrogen. The background and loaded spectra were obtained and subtracted to produce a difference spectrum. This difference spectrum showed no structure and had a total integrated intensity

TABLE 2: Summary of Dihydrogen Dosing Experiments and Observations

		H_2 dosing			
catalyst	cell[a]	*T*/K	dosing time/min	H/metal atomic ratio	neutron scattering observations
Pt/C	annular	77	5	0.35	H_2 rotor
Pt/C	annular	293	5	0.35	no H
Pt/C	annular	500	2200	0.74	H/C riding modes
Pt/C	standard	77	5	0.35	H_2 rotor
Pt/C	standard	293	30	0.27	H/C and H/Pt riding modes
Ru/C	standard	293	5	1.5	H/C and Ru/C riding modes
PtRu/C	standard	293	10	0.6	H/C and Pt/C, Ru/C riding modes

[a] See Experimental Section. In the annular cell only carbon is in the neutron beam. In the standard cell the catalyst is in the neutron beam.

across the entire frequency range of zero, to within experimental error. No subtraction procedures were required for the model compounds.

Results and Discussion

Our aim was to identify hydrogenic species on the catalysts and the carbon support, in particular to seek evidence, if any, for spillover hydrogen, We describe first the experimental INS spectra of the fast and slow hydrogen dosed catalysts and carbon. From the observed peak patterns we identify vibrational modes due to H associated with the metal and carbon components of the catalysts. We then assign the spectra with reference to the spectrum of the model compound coronene and the computed INS spectra. We exploit the graphite and coronene spectra in two ways. First, we pinpoint certain features of the spectra common to the H-dosed catalysts and to graphite and coronene. These features in common lead us to conclude that we are observing certain carbon modes enhanced by hydrogen: the so-called riding modes of hydrogen on carbon. That we see these modes is direct evidence for spillover of hydrogen. We do not, of course, expect a direct correspondence with the graphite spectrum, since the graphite spectrum comprises both bulk and surface modes. As we shall see, the coronene spectrum is a better representation of the surface modes.. In the latter part of the paper, we undertake a detailed analysis of the experimental and computed INS spectra of coronene, regarded as a molecular model of a graphite layer. We are then able to decide the probable location of at least part of the spillover hydrogen, namely at edge sites of graphitic carbon.

Hydrogen Uptake Experiments—Evidence for Spillover. The experiments are summarized in Table 2. When H_2 was adsorbed at 77 K by the catalyst in the standard cell and the annular cell, we saw the INS spectrum of the H_2 rotor. Therefore, dihydrogen had *not* dissociated. When a catalyst dosed with hydrogen at 77 K was allowed to warm to 293 K (or H_2 was adsorbed at 293 K), the spectrum of the H_2 rotor was *not* observed. With the standard cell (catalyst in the neutron beam) we observed neutron scattering (see below) from H atoms interacting with both the metal component of the catalyst and the carbon support. With the annular cell (only the carbon support in the neutron beam) the catalyst adsorbed dihydrogen at 293 K but there was no increase of neutron scattering from the central part of the annular cell; therefore, any spillover hydrogen had not diffused onto carbon in the central part of the annular cell. When the catalyst in the annular cell was heated to ~500 K, a further slow uptake of hydrogen was observed over a period of days. *The INS spectrum then showed hydrogen atoms on the carbon support*. The kinetics was consistent with slow diffusion of H atoms across the carbon, establishing equilibrium between hydrogen undergoing spillover and reverse spillover.[17]

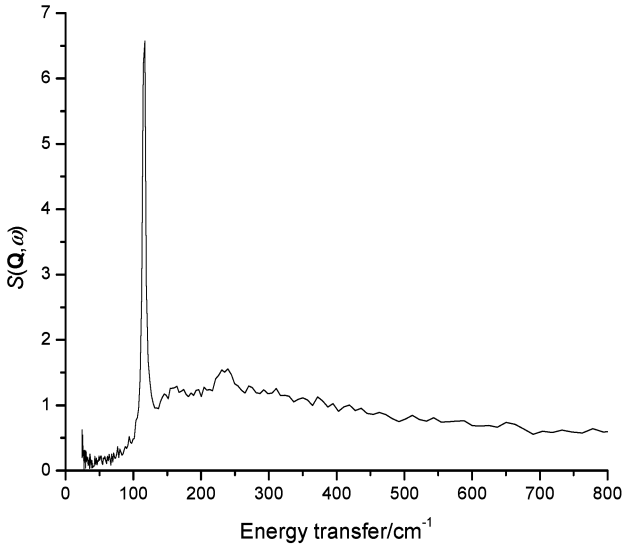

Figure 1. INS spectrum of H_2 adsorbed on carbon in the annular cell at 70 K. The peak is assigned to the H_2 rotor; see text. This peak was *not* present after warming or when H_2 was adsorbed by the catalyst at 293 K, showing that H_2 adsorption at 293 K is dissociative.

The INS spectra are described and assigned (with the aid of model compounds and computed spectra) in the following sections.

INS Spectrum after Low-Temperature Dihydrogen Adsorption on Pt/C—Molecular H_2. The INS spectra obtained after H_2 adsorption at 77 K using the annular cell with carbon in the central part and catalyst pellets at the edge showed the H_2 rotor peak at 120 cm^{-1};[6,7,20] see Figure 1. The H_2 peak was absent after warming and hydrogen adsorption at 293 K, evidently because the H_2 molecules had dissociated. Thus, the INS spectra provide *direct and unique evidence* of H_2 dissociative chemisorption.

INS Spectra of the Slow- and Fast-H-Dosed Catalysts and Carbon. Background spectra and the catalyst spectra are shown in Figure 2. For each catalyst adsorbed, hydrogen enhances the neutron scattering intensity. The difference spectra are shown in Figure 3. We consider that the effects are real, since the spectra are reproducible and, more significantly, the scattering intensity due to adsorbed hydrogen is proportional to the amount of hydrogen adsorbed (Figure 4). It is important to appreciate that the spectra of the H-dosed catalyts (Figure 3c−f) are *difference spectra*: the spectra of the catalysts and the container before hydrogen dosing (the background spectra) have been subtracted. The spectra are, therefore, due to hydrogen. Included in Figure 3 is the spectrum of coronene, showing carbon atom displacements only (see below) and so modeling a graphite layer.

H/C and H/M Riding Modes (M = Pt, Ru). In Figure 3 we observe a number of features common to the graphite spectra, the coronene spectrum, and the H-dosed catalyst spectra. For

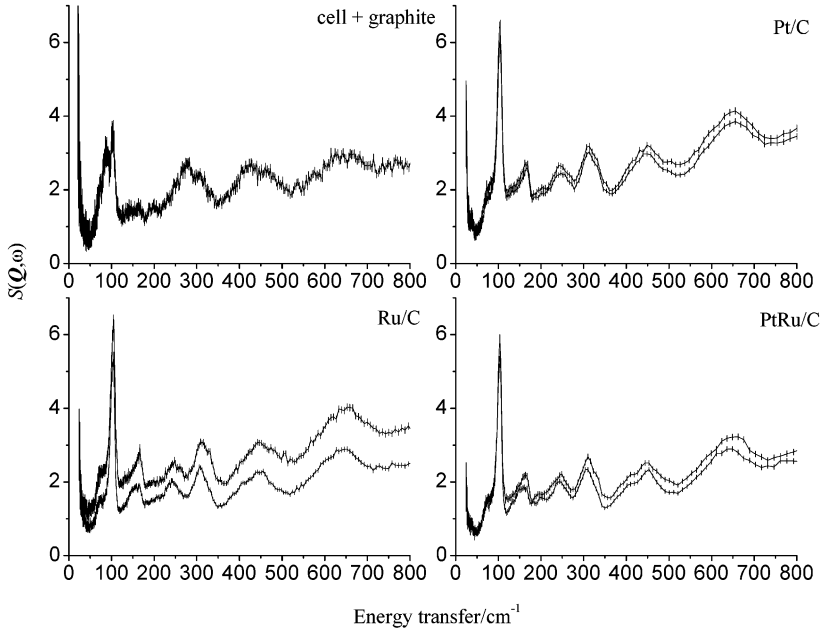

Figure 2. INS spectra of catalysts (lower curve) and hydrogen-dosed catalysts (upper curve) and the annular cell with graphite recorded on the ISIS TOSCA spectrometer at ~20 K. Error bars are shown as vertical lines.

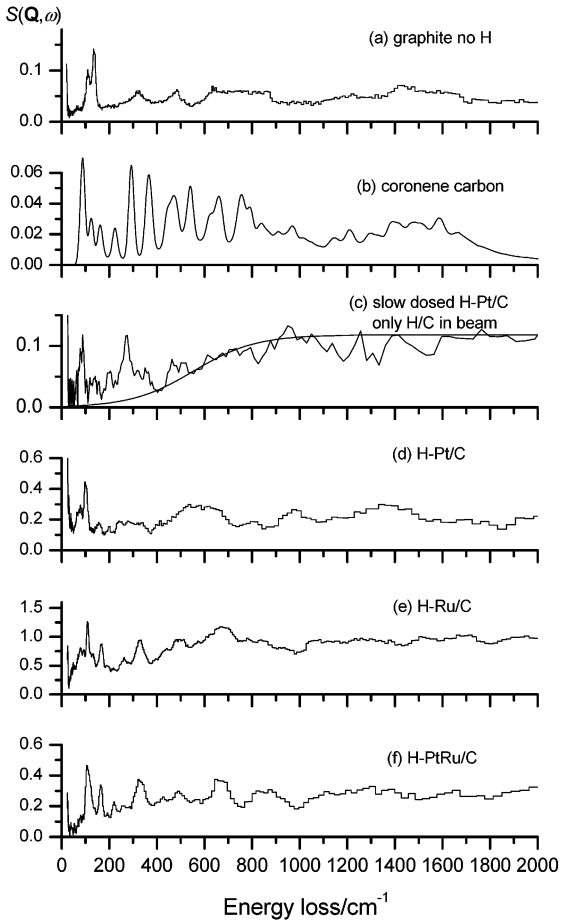

Figure 3. Inelastic neutron scattering spectra of (a) graphite replotted from ref 21, no H dosing; (b) coronene carbon modes, calculated (see p 22); (c) carbon support, annular cell, slow-H-dosed Pt/C catalyst (INS after dosing with H_2 at 500 K for 36 h); and (d−f) fast-H-dosed catalysts after dosing with H_2, background (steel container plus catalyst before hydrogen dosing) subtracted. In part c the continuous line is a sigmoidal fit to the higher energy scattering (see text).

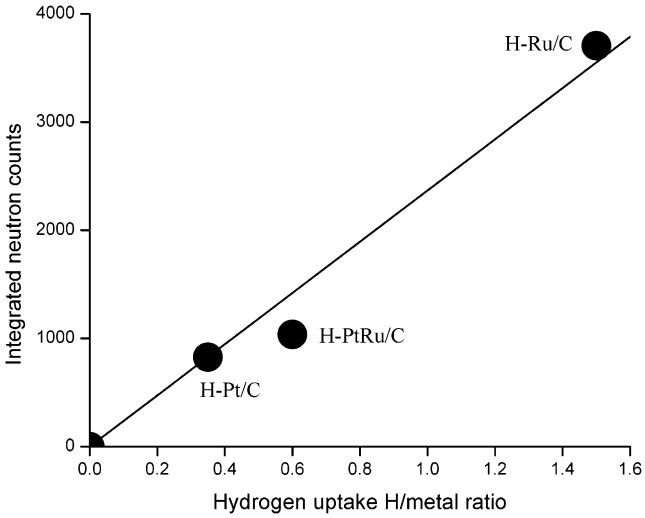

Figure 4. Integrated neutron scattering intensities from Figure 3 vs hydrogen uptake from Table 2. The line is the best straight line through the origin.

the catalysts these features appear in the background-subtracted spectra (Figure 3c−e) only after dosing with hydrogen. The result for the annular cell experiment (Figure 3c) is most significant. Here the only material exposed to the neutron beam is graphite in the central region of the annular cell. Moreover, in the H dosing experiment it is only when we have catalyst particles in the outer ring (and so not in the neutron beam) that we see the features of the spectra apparent in the figure. If we dose the cell with hyhdrogen without having catalyst in the cell, then these additional features are absent. The difference spectrum has constant zero intensity. Thus, the spectrum of Figure 3c is due to dissociated hydrogen located on graphite—conclusive evidence for spillover. It is also apparent from the spectra of Figure 3c compared with Figure 3a and b that there are a number of peaks in common, most obsviously in the region below 500 cm^{-1}. We assign the peaks later. Here we emphasize that the graphite and coronene spectra are due to modes involving displacements of carbon atoms. (The graphite has not been dosed with hydrogen.) We conclude that the peaks in Figure 3c are similarly due to carbon atom displacements and that we observe these displacements in the difference spectra

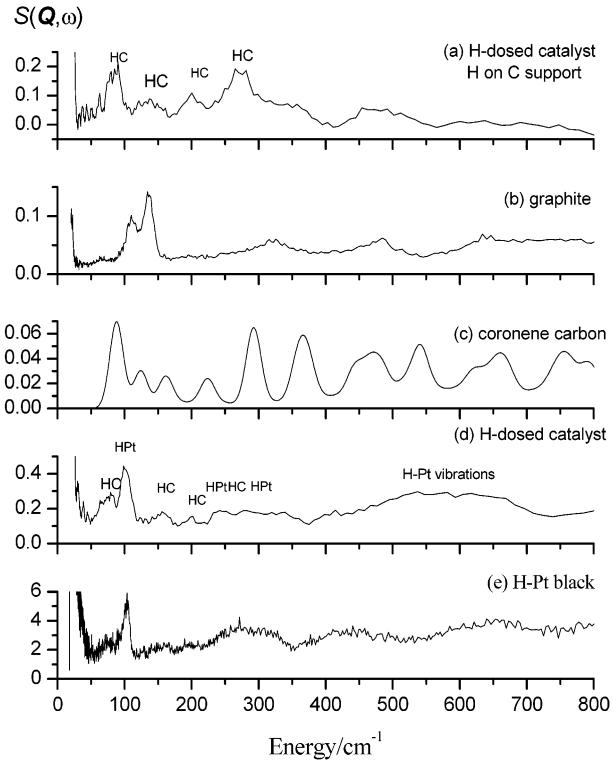

Figure 5. INS spectra of (a) slow-H-dosed Pt/C in the annular cell, that is, with only carbon and H thereon in the neutron beam; (b) graphite replotted from ref 21; (c) calculated carbon-only coronene spectrum, that is, H modes suppressed; (d) fast H-dosed catalysts in the standard cell, that is, with the catalyst and H thereon in the neutron beam; and (e) Pt black reduced, evacuated, and dosed with hydrogen. Peaks labeled HC are due to riding modes of H on carbon, and those labeled HPt are due to riding modes of H on Pt (peaks additional to those observed for carbon and H on carbon). Note that the H−Pt peak of the catalyst at ∼100 cm^{-1} corresponds to the strong peak in the Pt black spectrum.

because of the neutron scattering intensity enhancement due to H atoms riding on the carbon atoms: the riding modes.

In comparison with the cases of graphite and the model graphite layer, we might be tempted to assign peaks below 200 cm^{-1} to H−C riding modes. However, in this region there is a strong peak in the INS spectrum of Pt black (102 cm^{-1}).[22] The peaks in the spectra of the catalysts could, therefore, be assigned to H−Pt or H−Ru riding modes. To aid the analysis of the spectra, we plot in Figure 5 expanded spectra of the carbon and H/PtC catalysts in the region below 400 cm^{-1} and the spectrum of platinum black..The *additional* scattering from the H/PtC catalyst compared with carbon, seen as peaks labeled HPt in Figure 5, is in the region of Pt lattice vibrations, and these peaks are assigned to riding modes of H on Pt. Note that the H riding mode on Ru (Figure 3e) is shifted by ∼ +10 cm^{-1} relative to H on Pt, consistent with the greater strength of the Ru−Ru bond compared with the Pt−Pt bond (cf. enthalpies of atomization:[23] Ru, 651 kJ mol^{-1}; Pt, 566 kJ mol^{-1}). Thus, in the INS spectra of the H-dosed catalysts we see strong evidence for H/Pt or H/Ru and also H/C interactions, that is, spillover H.

INS of Slowly Diffused Spillover Hydrogen after Dosing at 500 K. The INS spectrum from carbon in the central part of the annular cell due to scattering from the slowly diffused spillover H, after subtracting the spectrum of the carbon support and the cell, is shown in Figure 3c.

We observe (1) a sigmoidal increase of scattering intensity between ∼500 and 1000 cm^{-1} shown by the continuous line,

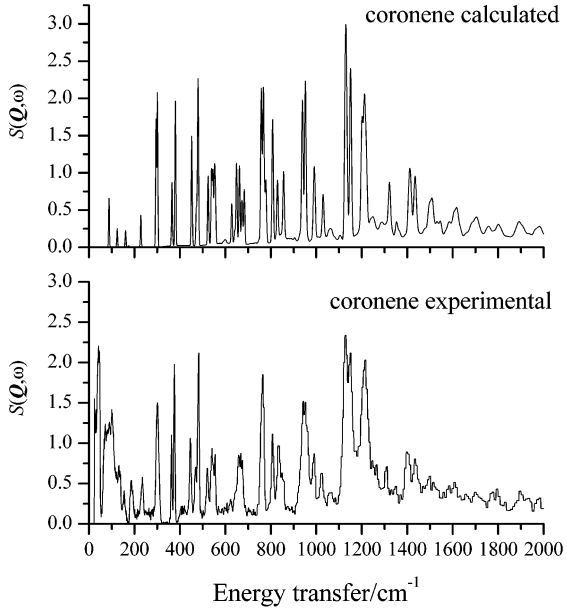

Figure 6. Coronene INS spectra, experimental and calculated. Vibrational spectrum computed with the Gaussian98 program (basis set 6-311G). Eigenvalues and eigenvectors input to the a-Climax program to compute the INS spectrum. See text.

(2) a continuum at energy transfer greater than ∼1000 cm^{-1} typical of scattering from weakly bound, mobile H atoms,[24] and (3) low energy peaks: riding modes of H on carbon (cf. peaks labeled H/C in Figure 5). The INS once again provides evidence for H spillover.

Experimental and Computed INS Spectrum of Coronene. To interpret the INS spectra of hydrogen-dosed metal/carbon catalysts, we have recourse to the spectra of model compounds and to calculated spectra. An appropriate model compound is coronene, $C_{24}H_{12}$ (**1**), which has a delocalized aromatic structure

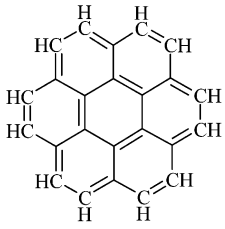

1

like a fragment of a graphite layer terminated with H atoms. Coronene may be taken as a one-layer cluster model of the graphite (0001) basal surface.[25] The 12 hydrogen atoms passivate the terminal dangling bonds of the C_{24} cluster; they are well away from the central ring. We have measured and calculated the INS of coronene.The vibrational spectrum of coronene (**1**) was calculated using Gaussian 98 with the B3LYP functional and the 6-311G basis set.[26] The vibration frequencies and atom eigenvectors were input to the a-Climax program[27] to calculate the INS spectrum. Following conventional practice, the calculated spectrum was scaled by 0.83.[28] The spectra are shown in Figure 6.

The agreement between the experimental and calculated spectra is good. We are, therefore, confident in our calculations on these and similar systems. Recently, Papanek et al.[29] in a neutron scattering study of disordered carbon anode materials reported the INS spectrum of coronene**.** The two sets of spectra

TABLE 3: Inelastic Neutron Scattering Spectra below 400 cm^{-1}: Positions/cm^{-1} and Assignments[a] of HPt Riding Modes and the HC Modes Diagnostic of Spillover[b]

coronene[c]	graphite				Pt	H/Pt/C	H/Ru/C	H/Pt/Ru/C	
INS	INS[d]	IR[e]	Raman[f] calc		INS	INS	INS	INS	
calc	exp	exp	bulk	layer	exp	exp	exp	exp	assignment[g]
90									ring def out-of-plane
	110								ring def out-of-plane
						80	80	80	ring def out-of-plane: HC riding
						100	110	105	HM riding
					102				Pt lattice, Pt black
125	135	130	136	136					ring def out-of-plane
						135			ring def out-of-plane: HC riding
160									ring def out-of-plane
						155	170	165	HM riding
						200	195	195	ring def out-of-plane: HC riding
225									ring def out-of-plane
					250				Pt lattice
						240	260	255	HM riding
						270	265	255	ring def out-of-plane: HC riding
290	320					340	325	325	ring def out-of-plane: HC riding
365									ring def out-of-plane

[a] This work unless otherwise referenced. [b] H_2 dosed catalyst difference spectra, that is, sample container and catalyst before dosing is subtracted. Fast H_2 uptake. Catalysts in neutron beam. [c] Calculated carbon atom displacement modes: see text. [d] Reference 21. [e] Reference 33. [f] References 31 and 34. [g] Abbreviations: def, deformation; HM, hydrogen riding on Pt or Ru; HC, hydrogen riding on carbon.

are in good agreement, although the TOSCA spectra are somewhat better resolved and we attend more to the low energy region.

For coronene there are 102 fundamental internal modes. Our interest here is not so much in the detailed assignments as in identifying those modes associated with carbon atom displacements that may aid in the interpretation of the spectrum of spillover H on carbon. These features of the spectra are pertinent: (1) Out-of-plane bending and torsional modes of the coronene ring, 90−300 cm^{-1}. These are predominantly displacements of the edge carbon atoms. The hydrogen atoms move with the carbon atoms, since they are naturally entrained in these normal modes. We shall see that these are the same modes that are amplified by spillover H on the carbon supports of our catalysts. The low wavenumber modes of the experimental and computed spectra of naphthalene have similarly been assigned.[30] (2) In-plane C−C stretching and breathing modes of the coronene rings (1000, 1230, 1400, 1450, 1600 cm^{-1}). These are equivalent to the surface modes of a graphite layer. (3) C−H bending modes: out-of-plane, 980−1020 cm^{-1}; in-plane, 1100−1700 cm^{-1}.

Structures and Vibrational Spectra of Amorphous Carbon and Graphite. Our concern is the detection and characterization of hydrogenic species on our carbon-supported catalysts rather than the structure of the carbon support. However, we include some discussion of the vibrational spectrum of graphite in view of the amplification of the surface modes of graphite by adsorbed hydrogen.

An amorphous carbon is graphitic rather than diamond-like. For example, the dominant peak in the Raman spectrum of amorphous carbon (1581 cm^{-1}) is satisfactorily calculated (1591 cm^{-1}) for a structure consisting of planar carbon (i.e., graphitic) with ∼10% tetrahedral carbon.[31] The occasional tetrahedral carbon allows changes in orientation of the graphitic planes. The INS of graphite has been measured, and the bulk and surface modes of graphite slabs have been calculated from a lattice dynamics simulation, which permitted an assignment of the modes.[32] The computational modeling assumed a stacked layer structure of the graphite crystal with the layers infinitely extended in the directions parallel to the basal planes.[32] The surface modes are those of the basal plane. Sites at right angles to the basal plane, edge sites, where the layers are truncated, are necessarily not included in the computational modeling. We shall see that as a consequence of hydrogen spillover the edge sites become decorated with H atoms.

In using coronene to model the INS spectrum of a graphite layer, we can investigate the edge sites through the low wavenumber vibrational modes due to displacements of edge carbon atoms. In the a-CLIMAX program it is possible to suppress H modes by assigning an infinite mass and zero scattering cross section to H atoms; the resulting spectrum, see Figure 5c below, is the spectrum due to the carbon atoms and so approximates the modes of a graphite layer.

Positions of the main diagnostic peaks and assignments are in Table 3.

Vibrational Modes of Coronene and Graphite and Comparison with the Hydrogen-Dosed Catalysts. The vibrational Raman and infrared spectra of coronene, graphite, and carbon have been reported; see Table 2. For single-crystal hexagonal graphite (space group D_{6h}^4) there is a Raman peak at 1582 cm^{-1} (E_{2g}): the so-called G-mode.[35] In the INS spectrum (Figure 3) the corresponding peak is part of the broad band near 1500 cm^{-1}. The INS is the complete density of states and is not restricted to the Brillouin zone center modes, as are the infrared and Raman spectra. The eigenvector involves in-plane bond stretch motions of pairs of sp^2 carbon atoms. For disordered graphite a peak is observed at 1355 cm^{-1}, the A_{1g} in-plane symmetric breathing mode of the six-member aromatic rings, the D-mode, which is forbidden in perfect graphite[34−36]

A common force field for graphite and polycyclic hydrocarbons (including coronene) has been proposed.[25] The two kinds of motion of carbon-sp^2 aromatic systems, which produce strong Raman lines in the spectra of graphite and the hydrocarbons, are the in-phase stretching and shrinking of the horizontal bonds (E_{2g} of graphite, 1581 cm^{-1}, coronene, 1620 cm^{-1}) and the ring breathing mode (A_{1g} of graphite, 1339 cm^{-1}, coronene, 1350 cm^{-1}).

In our INS spectrum of graphite the E_{2g} mode appears as a shoulder near 1600 cm^{-1} on a broad band centered at ∼1450 cm^{-1}, the A_{1g} mode. These are internal modes of the graphite

layer. The corresponding modes, in-plane C−C stretching and breathing modes, are seen in the INS spectrum of coronene (Figure 5).

The graphite modes that are enhanced and so observed in the spectra of the H-dosed catalysts (see Figure 5 and Table 2) are, by analogy with coronene, out-of-plane deformations and bending modes; see Table 2. Therefore, we have spillover H bound to the carbon particles at dangling bonds of edge sites. Note that the enhancement is more obvious for the Ru containing catalysts than for the Pt/C catalyst.

The low wavenumber prominent peaks of graphite (110, 136 cm^{-1}) are assigned by analogy with coronene (92, 130 cm^{-1}) to out-of-plane vibrations of edge carbons. Addition of H, as in coronene, or through H spillover, may shift this vibration to a lower wavenumber compared with the case of graphite. Therefore, in the spectra of the H-dosed catalysts, we assign the low energy peak at ∼80 cm^{-1} to a riding mode of H on carbon.

We show the INS spectra of the H-dosed catalysts and graphite in Figure 3. We see that the graphite band at ∼1450 cm^{-1} is absent from the spectra of the H-dosed catalysts. This is because we have subtracted out the carbon spectrum from the catalyst spectra. That the 1450 cm^{-1} band is not observed is also evidence that hydrogen is not bound to the graphitic basal plane region of the carbon supports—were this to have been so, the in-plane modes would have been enhanced in the INS spectra of the catalysts.

The Continuum. We attribute the enhanced scattering above ∼1000 cm^{-1} to a layer of free hydrogen atoms on the carbon support. The sigmoidal form of the plot (Figure 3) can be accounted for by a recoil process. We fit to an empirical sigmoidal function; the inflection value, 550 ± 20 cm^{-1} is a transition energy from the ground state of the H atom on the surface. The 1450 cm^{-1} graphite mode is not enhanced by the surface hydrogen because it is above this excitation threshold. We now justify this interpretation by computational modeling of the interaction of a H atom with graphite and calculating the energy barrier.

Computational Modeling of the Interaction of a H Atom with Graphite. Previously, the interaction of H atoms with the coronene ring has been investigated theoretically by density functional theory (DFT) calculations: the preferred binding site of a hydrogen atom is directly above a basal carbon atom.[25] We, and others,[11] have repeated and confirmed these calculations. We have now calculated with the periodic code CRYSTAL 98[37] the interaction energies of hydrogen atoms approaching binding sites on an idealized graphite slab. The interaction energy was calculated, as a function of distance, for a hydrogen atom approaching possible binding sites on a graphite slab: the atop site, that is, H directly above a C atom; the bridge site, that is, H at the midpoint between two carbon atoms; the hollow site, that is, H above the center of the C-6 hexagon. The interaction energies are plotted in Figure 7; the minima represent maxima in the binding energies. The preferred hydrogen binding site was the atop site. The interaction energies at the bridge site and the hollow site were less by 15 kJ/mol, and their potential well is more diffuse. The results, therefore, agree with those reported for cluster calculations of H on coronene,[25] that is, two adsorption regions separated by a barrier: a physisorption region and a chemisorption region. In the physisorption region, at ∼2.7 Å from the surface, there is no significant energy difference between the binding sites; this is a mobility channel. The H atom is free to move across the surface. We thus envisage a weakly bound and mobile precursor state of spillover hydrogen atoms leading to a state of more strongly bound hydrogen.

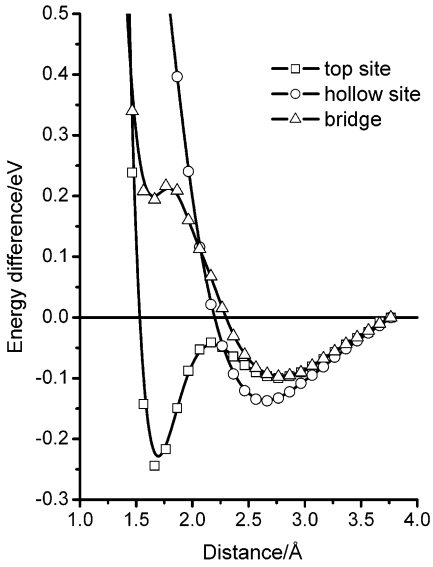

Figure 7. Interaction of H atom with sites on graphite (see text): interaction energy vs the vertical height of H above the surface. Periodic calculation with CRYSTAL 98, 6-31 G basis, supercell (2 × 2) × 2 unit cells.

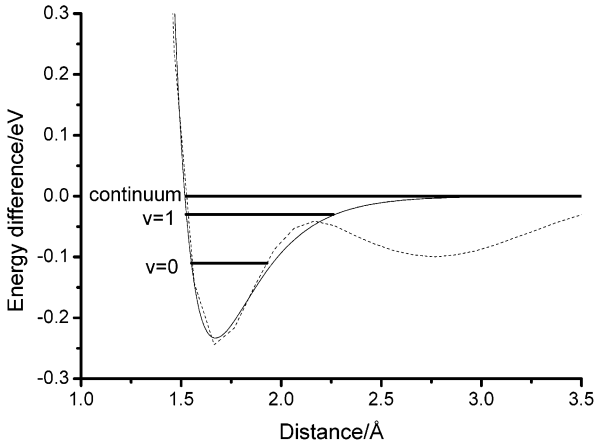

Figure 8. Interaction of H with graphite. Morse potential (full line) fitted to the interaction energy (broken line) for H approaching the atop site (cf. Figure 5) and vibrational energy levels.

The attractive part of the curve for adsorption on the atop site in Figure 7 was fitted to a Morse potential energy curve (Figure 8) to obtain the energy levels of the hydrogen atom and the possible transitions:

$$V(R) = -D_e \exp(-a(R - R_e))^2$$

where D_e is the depth of the potential minimum, R_e is the position of the minimum of the curve, and a is a constant. The best-fit parameters were $D_e = 0.2333$ eV, $a = 4.534$ $Å^{-1}$, and $R_e = 1.671$ Å. From the vibrational levels (Figure 8), we obtain a transition energy (0−1) of ∼610 cm^{-1}, in reasonable agreement with the experimental value of 550 cm^{-1}. The first excited state has energy close to, or above, the top of the barrier separating the on-top bound site from the mobility channel. The H atom wave function in the well will undoubtedly extend into this area, which should be regarded as a continuum across the entire surface.

Finally, we comment on how our concept of a quasi-continuum of physisorbed hydrogen relates to the free proton. The free proton wave function is continuous and three-dimensional and extends over the longest length scales. Proton

transport is a quantum mechanical event. The spillover hydrogen wave function exists in two forms, the mobile and the trapped forms. The trapped form can be described by a ground-state oscillator wave function localized over a carbon atom. In the mobile form the wave function exits, approximately, across the saddle points of an "egg-box" surface potential; it is two-dimensional and noncontinuous and extends only over short ranges. Surface diffusion of the spilled-over hydrogen proceeds by a series of, almost, classical hops from carbon trap to carbon trap. One could speculate that the ideal free proton wave function could never be truly achieved within the materials for which it has been proposed. Further, one could conclude that it was more likely to be two-dimensional and noncontinuous and exist over only modest length scales. The quantum mechanical proton transport would then come to resemble classical diffusion. However, this speculation is unnecessary, and we make no comparison between the free proton and spillover hydrogen.

Conclusions

The inelastic neutron scattering (INS) spectra of Pt/C, Ru/C, and PtRu/C fuel cell catalysts dosed with hydrogen have been determined in two sets of experiments: with the catalyst in the neutron beam and, using an annular cell, with carbon in the beam and catalyst pellets at the edge of the cell excluded from the beam. The vibrational modes observed in the INS spectra have been assigned with reference to the INS of a polycyclic aromatic hydrocarbon, coronene, as a molecular model of a graphite layer, and with the aid of computational modeling. Two forms of spillover hydrogen have been identified: H at edge sites of a graphite layer (formed after ambient dissociative chemisorption of H_2), and a weakly bound layer of mobile H atoms (formed by surface diffusion of H atoms after dissociative chemisorption of H_2 at 500 K). The INS spectra exhibit characteristic riding modes of H on carbon and on Pt or Ru. In these riding modes H atoms move in phase with vibrations of the carbon and metal lattices. The lattice modes are amplified by neutron scattering from the H atoms attached to lattice atoms. Uptake of hydrogen, and spillover, is greater for the Ru containing catalysts than for the Pt/C catalyst. The INS experiments have thus directly demonstrated H spillover to the carbon support of these metal catalysts.

Acknowledgment. We thank EPSRC for funding this research, the Leverhulme Trust for the award of an Emeritus Fellowship (P.C.H.M.), the Rutherford Appleton Laboratory for neutron beam time, and Johnson Matthey for the loan of catalysts.

References and Notes

(1) Paal, Z., Menon, P. G., Eds. *Hydrogen Effects in Catalysis*.; Marcel Dekker: New York, 1988.

(2) Pajonk, G. M. *Appl. Catal. A* **2000**, *202*, 157.

(3) (a) Conner, W. C. *Stud. Surf. Sci. Catal*. **1993**, *77*, 61. (b) Millar, G. J.; Rochester, C. H.; Bailey, S.; Waugh, K. C. *J. Chem. Soc., Faraday Trans.* **1993**, *89*, 1109. (c) Salzer, R.; Dressler, J.; Steinberg, K. H.; Roland, U.; Winkler, H.; Klaeboe, P. *Vib. Spectrosc.* **1991**, *1*, 363.

(4) (a) Baumgarten, E.; Maschke, L. *Appl. Catal. A, Gen.* **2000**, *202*, 171. (b) Liu, W. J.; Wu, B. L.; Cha, C. S. *J. Electroanal. Chem.* **1999**, *476*, 101. (c) Srinivas, S. T.; Rao, P. K. *J. Catal.* **1998**, *179*, 1. (d) Badenes, P.; Daza, L.; Rodriguez-Ramos, I.; Guerrero-Ruiz, A. *Stud. Surf. Sci. Catal*. **1997**, *112*, 241. (e) Bittner, E.; Bockrath, B. *J. Catal*. **1997**, *170*, 325. (f) Borisov, Y. A.; Zolotarev, Y. A.; Laskatelev, E. V.; Myasoedov, N. F. *Russ. Chem. B* **1997**, *46*, 407. (g) Menendez, J. A.; Radovic, L. R.; Xia, B.; Phillips, J. *J. Phys. Chem.* **1996**, *100*, 17243. (h) Srinivas, S. T.; Rao, P. K. *J. Catal.* **1994**, *148*, 470. (i) Rodriguez, N. M.; Baker, R. T. K. *J. Catal.* **1993**, *140*, 287. (j) Reddy, B. M.; Srinivas, S. T.; Rao, P. K. *Indian J. Chem., A: Inorg., Bio-inorg., Phys., Theor. Anal. Chem.* **1992**, *31*, 957.

(5) Mitchell, P. C. H. *Acta Phys. Hung.* **1994**, *75*, 131.

(6) Mitchell, P. C. H.; Parker, S. F.; Tomkinson, J.; Thompsett, D. *J. Chem. Soc., Faraday Trans.* **1998**, *94*, 1489.

(7) Ramirez-Cuesta, A. J.; Mitchell, P. C. H.; Parker, S. F. *J. Mol. Catal., A: Chem*. **2001**, *167*, 217.

(8) Albers, P.; Auer, E.; Ruth, K.; Parker, S. F**.** *J. Catal.* **2000**, *196*, 174.

(9) Nielsen, M.; McTague, J. P.; Ellenson, W. *J. Physique* **1977**, *38*, C4.

(10) Jeloaica, L.; Sidis, V. *Chem. Phys. Lett.* **1999**, *300*, 157.

(11) (a) Froudakis, G. E. *J. Phys.: Condens. Matter* **2002**, *14*, R453. (b) Ferro, Y.; Marinelli, F.; Allouche, A. *J. Chem. Phys.* **2002**, *116*, 8124. (c) Sha, X. W.; Jackson, B.; Lemoine, D. *J. Chem. Phys.* **2002**, *116*, 7158. (d) Sha, X. W.; Jackson, B. *Surf. Sci.* **2002**, *496*, 318. (e) Arellano, J. S.; Molina, L. M.; Rubio, A.; Alonso, J. A. *J. Chem. Phys.* **2000**, *112*, 8114.

(12) Besperstov, N. N.; Muzychka, A. Yu.; Natkaniec, I.; Nechitailov, P. B.; Sheka, E. F.; Shitikov, Yu. L. *Sov. Phys. JETP* **1989**, *69*, 989.

(13) Carneiro, K. *J. Phys.* **1977**, *38*, C4−1.

(14) Thomas, R. K. In *Molecular Spectroscopy*; Barrow, R. F., Long, D. A., Sheridan, J., Eds.; A Specialist Periodical Report, Vol. 6; The Chemical Society: London, 1978; p 312.

(15) Preuss, E.; Wuttig, M.; Sheka, E.; Natkaniec, I.; Nechitaylov, P. *J. Electron. Spectrosc. Relat. Phenom*. **1990**, *54*, 425.

(16) Howard, J.; Waddington, T. C.; Wright, C. J. *J. Chem. Phys.* **1976**, *64*, 3897 (L).

(17) Ramirez-Cuesta, A. J.; Mitchell, P. C. H.; Parker, S. F.; Tomkinson, J.; Thompsett, D. *Stud. Surf. Sci. Catal.* **2001**, *138*, 55.

(18) Bowden, Z. A.; Celli, M.; Cilloco, F.; Colognesi, D.; Newport, R. J.; Parker, S. F.; Ricci, F. P.; Rossi-Albertini, V.; Sacchetti, F.; Tomkinson, J.; Zoppi, M. *Physica B* **2000**, *276*, 98.

(19) *Origin User's Manual*, Version 6; Microcal Software, Inc.: 1999.

(20) Ramirez-Cuesta, A. J.; Mitchell, P. C. H.; Parker, S. F.; Barrett, P. A. *Chem. Commun*. **2000**, 1257.

(21) Walters, J. K.; Newport, R. J.; Parker, S. F.; Howells, W. S. *J. Phys.: Condens. Matter* **1995**, *7*, 10059. See also ISIS Database of Inelastic Neutron Scattering Spectra at http://www.isis.rl.ac.uk/molecularSpectroscopy.

(22) Ramirez-Cuesta, A. J.; Mitchell, P. C. H.; Parker, S. F.; Tomkinson, J. Unpublished INS spectrum.

(23) *CRC Handbook of Chemistry and Physic*s, 80th ed.; Lide, D. R., Ed.; 1999−2000; Section 9, Table 2: enthalpy of formation of gaseous atoms from elements in their standard states.

(24) Fillaux, F.; Cachet, C. H.; Ouboumour, H.; Tomkinson, J.; Levy-Clement, C.; Yu, L. T. *J. Electrochem. Soc*. **1993**, *140*, 585.

(25) (a) Mapelli, C.; Castiglioni, C.; Zerbi, G.; Mullen, K. *Phys. Rev. B* **1999**, *60*, 12710. (b) Ruuska, H.; Pakkanen, T. A. *J. Phys. Chem. B* **2001**, *105*, 9541.

(26) *Gaussian 98*, Rev A 6; Gaussian Inc.: 1998.

(27) Tomkinson J.; Ramirez-Cuesta, A. J.; Parker, S. F.; Champion, D. *aCLIMAX, A Users Guide to Version 3.0*; ISIS Facility, Rutherford Appleton Laboratory, CLRC: Chilton OX11 0QX, U.K.

(28) Foresman, J. B.; Frisch, A. *Exploring Chemistry with Electronic Structure Methods*, 2nd ed.; Gaussian, Inc.: Pittsburgh, PA, 1996; p 64.

(29) Papanek, P.; Kamitakahara, W. A.; Zhou, P.; Fischer, J. E. *J. Phys.: Condens. Matter* **2001**, *13*, 8287.

(30) Bokhenkov, E. L.; Natkaniec, I.; Sheka, E. F. *Sov. Phys. JETP* **1976**, *43*, 536.

(31) Beeman, D.; Silverman, J.; Lynds, R.; Anderson, M. R. *Phys. Rev. B* **1984**, *30*, 870.

(32) de Rouffignac, E.; Alldredge, G. P.; de Wette, F. W. *Phys. Rev. B* **1981**, *23*, 4208.

(33) Bekhterev, A. N. *Opt. Spektrosk.* **1986**, *60*, 647.

(34) Jawhari, T.; Roid, A.; Casado, J. *Carbon* **1995**, *33*, 1561.

(35) Ferrari, A. C.; Robertson, J. *Phys. Rev. B* **2000**, *61*, 14095.

(36) Doyle, T. E.; Dennison, J. R. *Phys. Rev. B* **1995**, *51*, 196.

(37) Saunders, V. R. *Crystal 98 Users Manual*; 1998.